



# Advanced Synthesis & Catalysis

## Accepted Article

**Title:** Tartramide Ligands for Copper-Catalyzed N-Arylation at Room Temperature

**Authors:** Xuerui Ma and Robert Davies

This manuscript has been accepted after peer review and appears as an Accepted Article online prior to editing, proofing, and formal publication of the final Version of Record (VoR). This work is currently citable by using the Digital Object Identifier (DOI) given below. The VoR will be published online in Early View as soon as possible and may be different to this Accepted Article as a result of editing. Readers should obtain the VoR from the journal website shown below when it is published to ensure accuracy of information. The authors are responsible for the content of this Accepted Article.

**To be cited as:** *Adv. Synth. Catal.* 10.1002/adsc.202200174

**Link to VoR:** <https://doi.org/10.1002/adsc.202200174>

DOI: 10.1002/adsc.201((will be filled in by the editorial staff))

# Tartramide Ligands for Copper-Catalyzed N-Arylation at Room Temperature

Xuerui Ma<sup>a</sup>, Robert P. Davies<sup>a\*</sup>

<sup>a</sup> Department of Chemistry, Imperial College London, South Kensington, London SW7 2AZ, United Kingdom  
E-mail: r.davies@imperial.ac.uk

Received: ((will be filled in by the editorial staff))

Supporting information for this article is available on the WWW under <http://dx.doi.org/10.1002/adsc.201#####>.

**Abstract.** Readily accessible tartramide ligands have been demonstrated to promote copper-catalysed N-arylation under mild conditions. In addition, the coupling protocol employs cheap and readily available pre-catalyst, ligand, and base (NaOH), and overcomes many current limitations often associated with Ullmann coupling: it can be run with low catalyst loadings, does not require the use of excess amine, operates at room temperature, is fully homogeneous, and displays improved tolerance to air and moisture. Detailed kinetic studies using reaction progress kinetic analysis (RPKA) methods have provided insight into the factors influencing the reaction rate in terms of

impact of ligand structure, reactant / catalyst dependence and catalyst (in)stability. These kinetic insights have been used in a quality-by-design approach for further optimization of the reaction protocol. The reaction scope was extended to 22 examples, showing broad applicability for a wide range of substituted aryl iodides with both primary and secondary amines.

**Keywords:** Copper; Ullmann Reaction; C-N bond formation; kinetics, RPKA

## Introduction

Aryl amines are important building blocks for a wide range of pharmaceuticals,<sup>[1–3]</sup> natural products,<sup>[4]</sup> and materials.<sup>[5,6]</sup> Transition-metal catalyzed C-N bond formation, and in particular Pd-catalyzed Buchwald-Hartwig reactions, are one of the most widely utilized and powerful processes for synthesis of these building blocks. However, copper catalyzed amination (Ullmann coupling) has recently been the subject of growing interest due to the low cost and low toxicity of copper (and its commonly employed ligands), as well as its good functional group tolerance.<sup>[7]</sup> Over the last two decades, a large number of oxygen and nitrogen based ligands have been found to effectively promote copper-catalyzed C-N bond formation, with recent advances demonstrating much improved increases in catalyst turnover number and frequency,<sup>[8]</sup> and the ability to activate more challenging substrates such as aryl chlorides.<sup>[9]</sup> Despite this, room-temperature copper-catalyzed amination remains challenging with elevated temperatures (80 – 120°C) required in the majority of cases.<sup>[10]</sup> In addition, copper catalyzed processes can suffer from reproducibility issues as well as exhibiting high sensitivity to air and moisture.

Room-temperature Ullmann cross coupling was first reported by Shafir and Buchwald in 2006 employing CuI (5 mol%) and a  $\beta$ -diketone ancillary ligand (20 mol%) for coupling of aryl iodides with aliphatic amines.<sup>[11]</sup> A small number of other room temperature studies subsequently followed with variations in ancillary ligand and substrate, however copper loadings remained in the 5-20 mol% range.<sup>[12–15]</sup> A switch from inorganic to organic base was shown by Fu and Liu to give improved room temperature reactivity, although 10 mol% CuI was still required.<sup>[12]</sup> The use of organic bases also resulted in the formation of homogenous reaction mixtures, and this led us to use these as model systems for gaining improved kinetic and mechanistic data for copper catalyzed coupling processes.<sup>[13]</sup> More recently, we further improved the protocol for these organic base systems to give good conversions with sub-mol% CuI loading at room temperature.<sup>[14]</sup> However, the cost and hydroscopic nature of organic bases is likely to hinder their widespread uptake. A drive to discover new systems that offer comparable performance with cheaper and more accessible inorganic bases has led to the work reported herein.

Practical copper-catalyzed C-N bond formation at room temperature with inorganic bases still faces several key challenges including: i) high catalyst loadings ( $\geq 5$  mol%); ii) poor reproducibility (in part

associated with the heterogeneous nature of the reaction mixture); iii) high sensitivity to moisture and air; iv) requirement for an excess of amine (up to 3.0 equivalence) and base (generally 2.0 equivalence). In addition, there is a lack of detailed understanding on the role of the ancillary ligand and little in the way of directly comparative ligand performance data.

We herein report a general solution which attempts to address all these concerns together. The system has been developed through an initial condition screening, followed by mechanistic investigations using reaction progress kinetic analysis (RPKA) methodology. The optimized system has been extended to 22 examples in which aryl iodides are shown to undergo smooth coupling with a range of aliphatic and aryl amines using CuI pre-catalyst (1+ mol%) with the cheap, and readily accessible novel tartramide ligand, D-FurTA (**L5**) (2+ mol%). The protocol only uses a slight excess of amine (1.1 equivalence) and base (NaOH, 1.1 equivalence) in a fully homogeneous mixture at room temperature and shows improved tolerance to air and moisture.

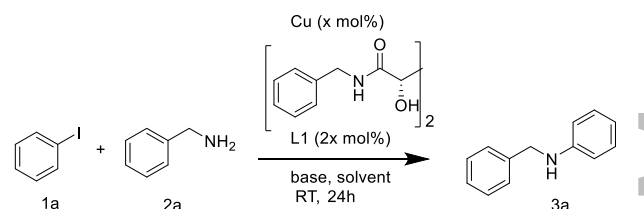
## Results and Discussion

**1. Initial Reaction Optimization and Auxiliary Ligand Evaluation.** This paper focusses upon the novel application of tartramide ligands in Ullmann amination. Tartramide derived ligands have previously been successfully employed in a number of titanium-catalyzed enantioselective reactions including Sharpless epoxidation,<sup>[15]</sup> Diels-Alder reactions,<sup>[16]</sup> and [2+2] cycloaddition reactions.<sup>[17]</sup> The reported ability of these ligands to stabilize high oxidation-state metals such as Ti(IV) attracted our attention given the putative importance of transient high oxidation state Cu(III) intermediates in Ullmann amination processes.<sup>[18,19]</sup> Moreover, tartramide ligands are readily accessible from cheap tartaric acid or tartrate starting materials, and show structural similarities to the powerful oxalic diamide ligands reported by Ma (also for Ullmann amination).<sup>[10]</sup> Initial screening was undertaken using tartaric acid dibenzyl amide (**L1**) as the ligand and benzylamine (**1a**) and iodobenzene (**2a**) as the substrates. The reactions were carried out at room temperature, and under air-free and dry conditions (Table 1). Initial reactions revealed both the base and solvent system to have a large influence on the reaction yield with diethylene glycol (DEG) in combination with an alkali hydroxide base (NaOH or KOH) giving the highest conversions (Entries 1-9). CuI was chosen as the copper pre-catalyst due to its low cost and full solubility in the studied reaction media. Replacing CuI with CuBr<sub>2</sub> as a soluble Cu(II) pre-catalyst led to no reaction (Entry 10).

Since close to quantitative yields were achievable with literature-typical catalyst loadings of 10 mol% CuI and 20 mol% ligand (Entry 9), lower catalyst loadings were also explored. Reducing catalyst loading to 5 mol% (10 mol% **L1**) or even 1 mol% (2 mol% **L1**) still gave close to quantitative conversion, although loadings below this led to a drop in observed yield (Entries 11-13).

In order to examine the robustness of this system towards air and moisture we also explored the use of undried (batch) commercial solvents and carried out the reaction open to the air. Under these conditions we were surprised to see no drop-off in yield (Entry 14). Deliberate introduction of water to the system (~11 equivalents), did lead to a modest decrease in yield to a still respectable 78% (Entry 15). In addition, in the presence of air the system was more sensitive to catalyst loading, with 65% yield observed for 5 mol% catalyst loading (Entry 16). Control experiments omitting ligand or copper gave no conversion to the desired cross-coupled product (Entries 17, 18).

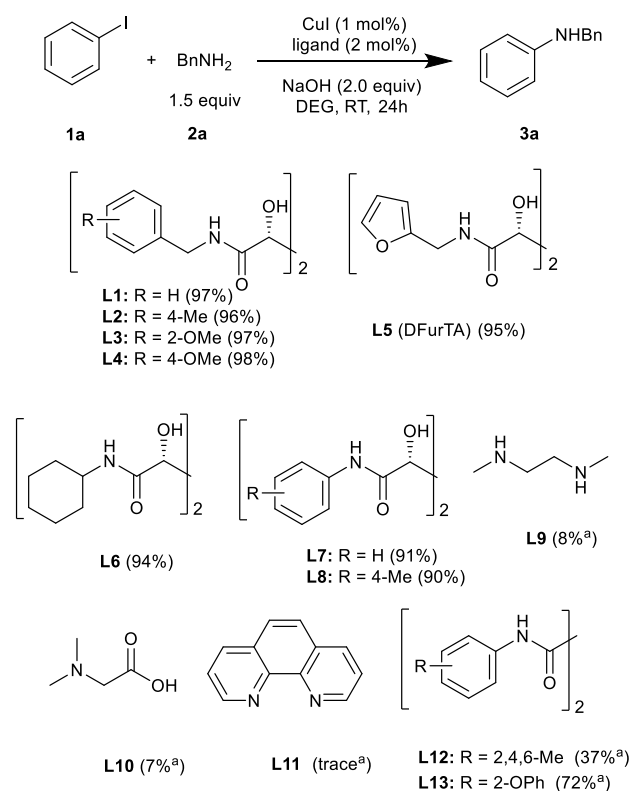
**Table 1.** Copper-catalyzed C-N bond formation of benzylamine (**1a**) and iodobenzene (**2a**): Reaction condition optimization<sup>a,b</sup>



Entry	Cu	Cu:L1 (mol%)	solvent	base	yield (%)
1	CuI	10:20	DMSO	K <sub>3</sub> PO <sub>4</sub>	trace
2	CuI	10:20	<sup>i</sup> PrOH	K <sub>3</sub> PO <sub>4</sub>	0
3	CuI	10:20	MeOH	NaOH	52
4	CuI	10:20	EtOH	NaOH	11
5	CuI	10:20	<sup>i</sup> PrOH	NaOH	13
6	CuI	10:20	DEG	K <sub>3</sub> PO <sub>4</sub>	90
7	CuI	10:20	DEG	DBU	7
8	CuI	10:20	DEG	KOH	97
9	CuI	10:20	DEG	NaOH	99
10	CuBr <sub>2</sub>	10:20	DEG	K <sub>3</sub> PO <sub>4</sub>	0
11	CuI	5:10	DEG	NaOH	99
12	CuI	1:2	DEG	NaOH	95
13	CuI	0.5:1	DEG	NaOH	53
14	CuI	10:20	DEG	NaOH	98 <sup>c</sup>
15	CuI	10:20	DEG:H <sub>2</sub> O (10:1)	NaOH	78 <sup>c</sup>
16	CuI	5:10	DEG	NaOH	65 <sup>c</sup>
17	CuI	10:0	DEG	NaOH	0
18	-	0:20	DEG	NaOH	0

<sup>a</sup> Reaction conditions: **1a** (1.0 mmol), **2a** (1.5 mmol), copper, ligand, base (2.0 mmol), solvent (2 mL), RT, 24h <sup>b</sup> Yields were determined by <sup>1</sup>H NMR using naphthalene as an internal standard. <sup>c</sup> under air, use of batch solvent

Encouraged by these results which demonstrated tatrarnide ligands to be efficient auxiliary ligands for room temperature Ullmann amination with good tolerance of air and small quantities of water, we expanded the range of tatrarnide ligands studied. The results are summarized in Scheme 1. As far as we are aware **L2-L6** are novel compounds; **L1**, **L7** and **L8** have been reported before in the literature.<sup>[20]</sup> Pleasingly, all the ligands facilitated excellent reactivity using just 1 mol% Cu loading (2 mol% ligand), giving almost quantitative conversions in the model cross-coupling reaction. To test if this class of ligand is unique under these conditions, other commonly employed ligands including recent examples of Ma's oxalamide ligands<sup>[10]</sup> (**L9 – L13**) were also evaluated. However only poor to moderate yields were obtainable using these alternative ligands even with ten times the catalyst loading (10 mol% Cu, 20 mol% ligand) – Scheme 1.



**Scheme 1.** Auxiliary ligands and corresponding yields. Reaction conditions: **1a** (1.0 mmol), **2a** (1.5 mmol), NaOH (2.0 mmol), DEG (2 mL), CuI (1 mol%, 0.01 mmol), **L1 – L8** (2 mol%, 0.02 mmol), RT, 24h, under N<sub>2</sub>. Yields were determined by <sup>1</sup>H NMR using naphthalene as an internal standard. <sup>a</sup>For **L9 – L13**, reactions were conducted with CuI (10 mol%, 0.1 mmol), and **L9 – L13** (20 mol%, 0.2 mmol).

**2 Kinetic Studies by Reaction Progress Kinetic Analysis (RPKA).** Kinetic studies on copper-catalyzed amination reactions are somewhat rare in the literature.<sup>[13,21]</sup> This can be attributed, at least in part, to the often-biphasic nature of these reactions – a result of the use of inorganic bases such as Cs<sub>2</sub>CO<sub>3</sub>, K<sub>3</sub>PO<sub>4</sub>, or K<sub>2</sub>CO<sub>3</sub> which have low solubility in most common reaction media. This gives rise to issues in reproducibility where the stirring method as well as the particle size, morphology, and surface area of the base can all influence the reaction kinetics.<sup>[22,23]</sup> Moreover, the reaction becomes inherently mass-transfer limited, thus observed kinetics are usually dominated by the rate of deprotonation of the amine rather than the activity of the copper catalyst. In contrast, our reaction system here employs a soluble base, NaOH (in DEG), which is not only more economical but also gives rise to a fully homogenous reaction mixture enabling simplified and straightforward kinetic analysis. Hence, we have undertaken a range of kinetic measurements to not only understand the system better, but also to enable a quality-by-design approach to catalyst development and optimization. In-situ reaction monitoring using calorimetry and NMR spectroscopy reveals ligand structure-activity relationships, identifies catalyst deactivation, and presents concentration dependences of reagents as well as catalysts.

Slightly modified reaction conditions were applied so that the cross-coupling reaction completed in approximately 2h (**[1a]** = 0.167 M, **[2a]** = 0.250 M, **[NaOH]** = 0.334M, 10 mol% CuI, 20 mol% **L1**) – see Supplementary Information for full details. The time profiles for this reaction using calorimetry and <sup>1</sup>H NMR are shown in Figure 1 with both methods giving consistent results. In addition, <sup>1</sup>H NMR analysis shows 100% conversion of phenyl iodide (**1a**) and ≥ 97% yield of the desired product (**3a**). Trace amount of benzene (≤ 1%) and phenol (≤ 2%) by-products were also observed. These have been previously reported as side products in Ullmann amination.<sup>[24–26]</sup> The calculated enthalpy of reaction,  $\Delta H_{rxn}$ , across all experiments was consistent within 5% error margin ( $\Delta H_{rxn} = 117.6 \pm 5.9 \text{ kJ mol}^{-1}$ ). The consistent reaction enthalpy and strong agreement in measured conversion with the <sup>1</sup>H NMR data (Figure 1) suggests that any heat flow released from dehalogenation and hydroxylation side reactions is negligible relative to that from the C-N cross coupling.

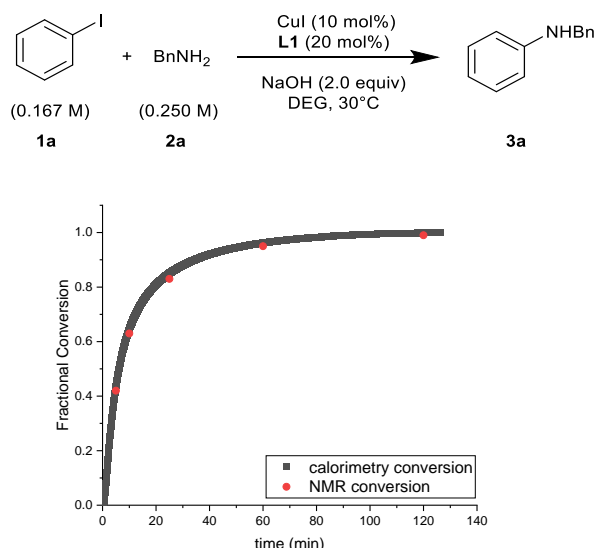


**Figure 1.** Comparison of conversion measured by NMR analysis to the conversion calculated from heat flow given by calorimetry

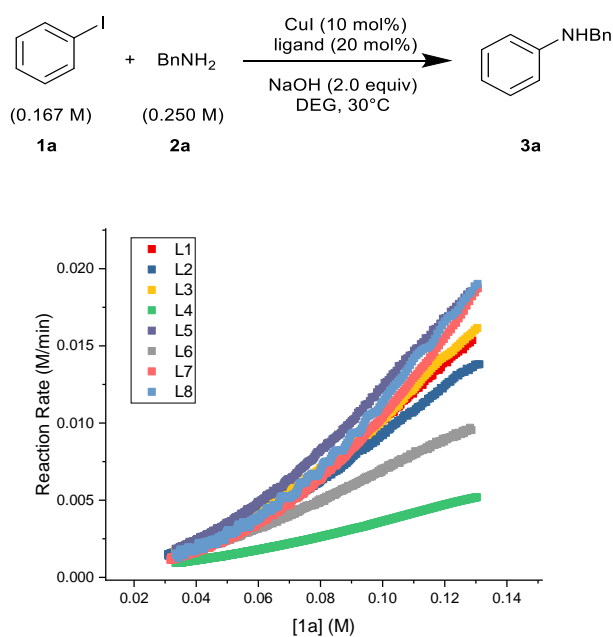


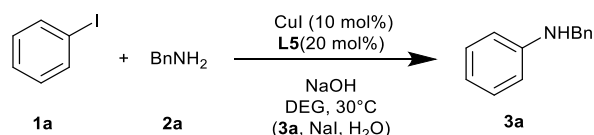
**Figure 2.** Graphical reaction equations for experiments using **L1** – **L8**. Progress of reaction runs from right to left.

**2.1. Ligand evaluation using kinetics.** In our initial ligand screening (Scheme 1), all new tartramide ligands gave similarly high conversions in the model reaction. Therefore, to better evaluate and compare the performance of these auxiliary ligands a series of kinetic experiments have been undertaken. Firstly, the rate vs  $[1]$  plots were collected under identical conditions in the presence of different auxiliary ligands (**L1** – **L8**). These results are shown in Figure 2 focusing on conversions between 20% - 75% for clarity (for full plots see Figure S3). Given the similarities in

yield data (Scheme 1), the variation in observed rates was perhaps surprising, with **L5** giving an approximately 4-fold enhancement of initial reaction rate compared to **L4**. This demonstrates the power of a kinetic approach to catalyst evaluation. It is also worth noting that although the phenyl tartramide ligands **L7** and **L8** exhibit a high initial rate, the kinetic curvature of these reactions is slightly larger than the others, suggesting other alternative pathways may also be occurring such as catalyst deactivation.

Based upon these results **L5** was identified as the best performing ligand for further kinetic studies and substrate scope explorations.

**2.2. Catalyst deactivation.** In order to probe catalyst stability over the course of the reaction, experiments were designed in accordance with the ‘same excess’ protocol of Reaction Progress Kinetic Analysis (RPKA) developed by Blackmond.<sup>[27]</sup> In a same excess experiment, ‘excess’, i.e. the difference in concentration between reactants (in this case, **1a**, **2a**, and NaOH) is fixed while the initial concentration chosen to start the reaction is different. As shown in Figure 3 the rate of the same excess experiment (trail 2, red) does not directly overlap with that of the standard experiment (trail 1, grey). The lower reactivity of trail 1 is indicative of the occurrence of either catalyst deactivation and/or product inhibition. Additional same excess experiments with deliberate addition of the reaction products were designed to probe this further. Addition of **3a** and NaI (trail 3, blue) gave direct overlap with trail 2 indicating no inhibition from these products and ruling out competitive coordination or reaction mixture conductivity change induced by **3a** and NaI. Addition of water however (trail 4, green) did lead to a small fall in reaction rate suggesting that in-situ generated water from reaction of the hydroxide base is likely to inhibit the catalytic process. The relatively small degree of deactivation with water additionally supports the robustness of the catalyst system as discussed in Section 2.1. The deviation between trail 4 and trail 1 in Figure 3 suggests that water inhibition is not the only cause of catalyst deactivation in this system. Other possible deactivation routes include disproportionation of the copper. This is also supported qualitatively by the observation of a pale green solution and red precipitate at the end of reaction, indicative of the formation of Cu(0) and Cu(II) species.<sup>[22]</sup>





Colour / Trail	[1a] <sub>0</sub> (mM)	[2a] <sub>0</sub> (mM)	[NaOH] <sub>0</sub> (mM)	[3a] <sub>0</sub> (mM)	[NaI] <sub>0</sub> (mM)	[H <sub>2</sub> O] <sub>0</sub> (mM)	obtained when using a weaker tetra-alkylammonium (or phosphonium) malonate base. <sup>[13,21]</sup> The use of the organic base in this prior work was shown to lead to the formation of off-cycle species from competitive multi-ligation of malonate to copper and subsequent irreversible disproportionation which masked the intrinsic rate dependence in amine and base. In contrast, an apparent zero-order dependence in amine and base here can be attributed to the use of NaOH, giving facile coordination / deprotonation of the amine in a pre-equilibrium step. The kinetically meaningful intermediate therefore contains the copper center, a deprotonated amine and the anionic auxiliary ligand. These observations parallel similar findings on Ullmann biaryl ether synthesis reported by Hartwig which were shown to be zero order in [ArOH] substrate, <sup>[28]</sup> and also has parallels in Pd-catalyzed aminations which have been shown to be zero order in [amine]. <sup>[29]</sup> Note that since a soluble, homogeneous reaction mixture was obtained for all experiments, mass-transfer effects due to limited solubility of base or amine cannot be inferred.
■ 1	167	250	334	0	0	0	
■ 2	117	200	284	0	0	0	
■ 3	117	200	284	50	50	0	
■ 4	117	200	284	0	0	50	
■ 5	117	200	284	50	50	50	

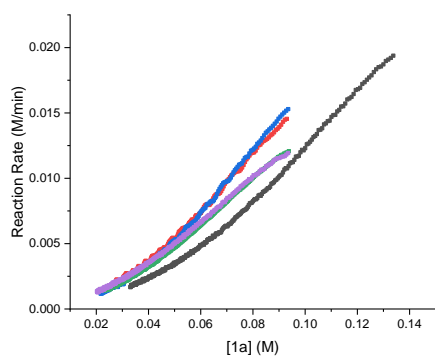


**Figure 3.** Graphical reaction equations for standard, same excess, and same excess with (by)product addition experiments.

**2.3. Rate dependence in substrates and catalyst.** The rate dependence of one substrate can be determined by varying the substrate concentration while keeping all other conditions the same (known as ‘different excess’ protocol).<sup>[27]</sup> As shown in Figure 4, overlap of the kinetic profiles was observed when varying the concentration of **2a** or NaOH, indicating apparent zero-order in both of these components.

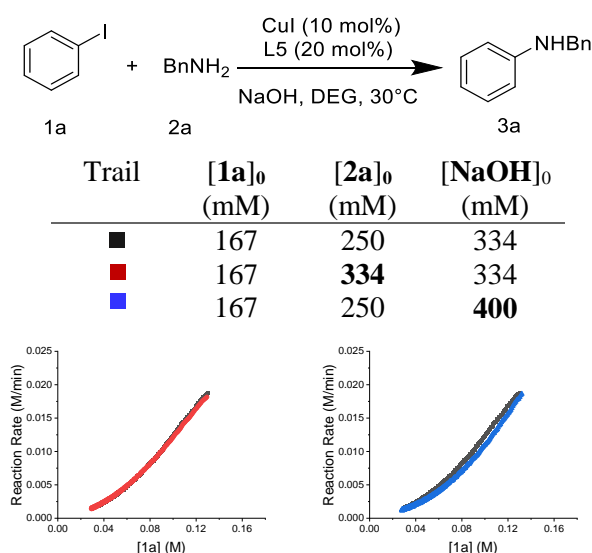


**Figure 4.** Graphical rate equations for different excess experiments regarding to **2a** and NaOH. See the Supporting Information for full graphical rate plots.

Previous studies in our group on Ullmann couplings have revealed first order dependence in amine and negative order in base, however these data were

symbol	[1a] <sub>0</sub> (mM)	[2a] <sub>0</sub> (mM)	[NaOH] <sub>0</sub> (mM)	[e] (mM)
■	167	250	334	83
■	125	250	334	125
■	83	250	334	167

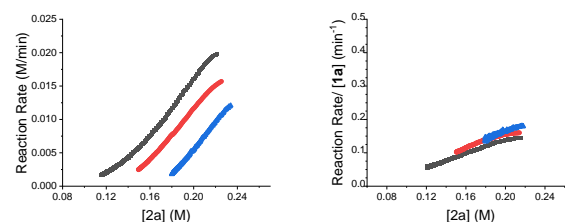


**Figure 5.** Graphical rate equations for different excess experiments regarding to **1a**; non-normalized (left) and normalized (right). See the Supporting Information for full graphical rate plots.

Different excess experiments in **1a** (Figure 5) show an approximately first-order rate dependence in aryl halide. This is in agreement with previous reports and is indicative aryl halide activation at the copper center being the rate-limiting step.<sup>[13,21]</sup>

Lastly, the effects of copper and auxiliary ligand loading on reaction rate are shown in Figures 6 and 7. The observed order of reaction in copper was

determined to be 0.9 (Figure 6). Deviation from catalyst order of unity is characteristic of catalyst deactivation, which is in accordance with the observed catalyst deactivation behavior in the ‘same excess’ experiments (Section 2.2).

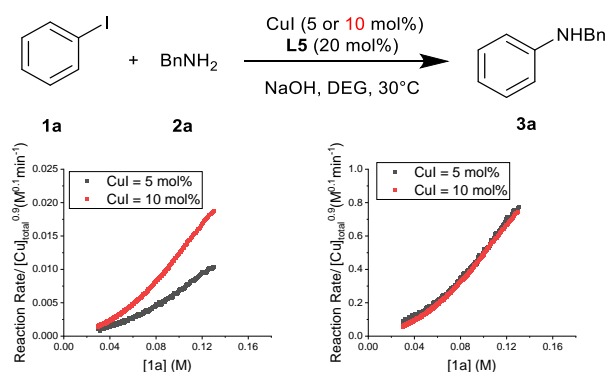


**Figure 6.** Non-normalized (left) and normalized by  $[\text{Cu}]_{\text{total}}^{0.9}$  (right) graphical rate equations for different excess in  $[\text{Cu}]_{\text{total}}$  experiments. See the Supporting Information for full graphical rate plots.

The reaction rate as a function of auxiliary ligand concentration was also examined. In the absence of ancillary ligand, the reaction exhibited 0% yield after 24 hours. However, increasing the ligand concentration up to 40 mol% relative to **1a** (400 mol% relative to CuI) reveals a positive non-linear relationship between the reaction rate and ligand concentration (Figure 7a). A plot of initial rate vs ligand loading (Figure 7b) is in excellent agreement with saturation behavior, fitting well with an equation of the form  $\text{rate} = A[\text{L5}]/(B + [\text{L5}])$  where A and B are variables and  $[\text{Cu}]_{\text{total}}$ , **1a** and **2a** are constant. Similar saturation behavior has previously been reported for diamine ligands in related N-arylation reactions.<sup>[30]</sup> Thus similar to these earlier studies, the catalytic species can be considered to be a LCuNRR' complex with too little ancillary ligand L leading to the formation of (off-cycle) inactive cuprates of the form  $[\text{Cu}(\text{NRR}')_2]$ .<sup>[30,31]</sup> The full dissolution of the CuI and **L5** rules out solubility playing a role in the saturation behavior.

The mode of coordination of the tetramide ligand to the copper centre remains undetermined with deprotonation and coordination from both amide NH and alcohol OH sites possible. Attempts to synthesise or isolate **L5CuI** or **L5Cu(amide)** type complexes for structural characterisation have proved unsuccessful to date. However, a feasible assumption is that the ligands will act as dianionic  $\text{L}_2\text{X}_2$  systems in which one of the LX units can be displaced to facilitate aryl iodide addition.

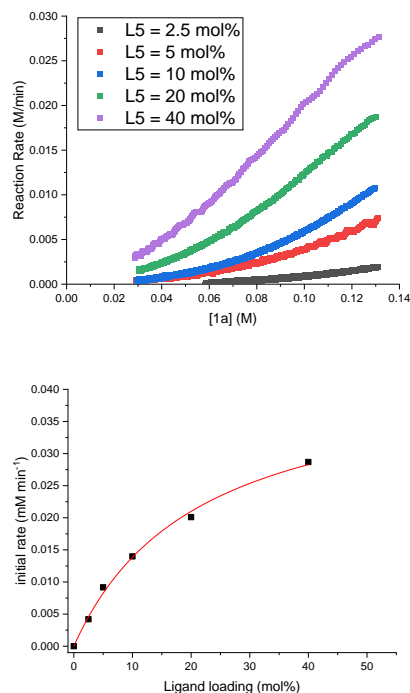
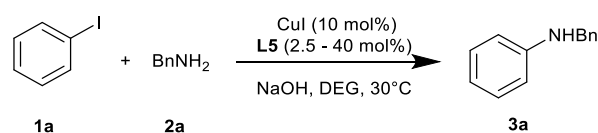
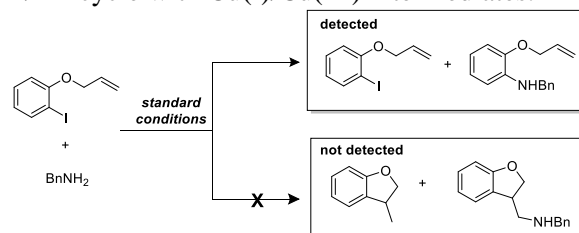


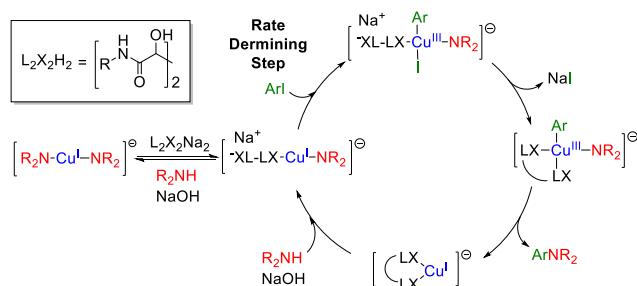
**Figure 7.** (top) Graphical rate equations for different excess experiments in terms of **L5** (bottom) plot of the initial rate versus the ligand loading shows a non-linear relationship. The curve was fitted by a non-linear least-squares equation:  $\text{rate} = A[\text{L5}]/(B + [\text{L5}])$  where  $A = 0.04332$ ,  $B = 21.2624$ , R-square value = 0.9965

**2.4. Halide activation studies.** To identify whether the coupling reaction proceed via a radical-based or an oxidative addition / reductive elimination (OA/RE) mechanism, radical clock experiments were conducted using 2-(allyloxy)iodobenzene as the substrate and radical probe. If the activation of aryl iodide occurs via a radical route, the free aryl radical will rapidly lead to a cyclisation via an extremely fast 5-exo-trig process. However, GC-MS and  $^1\text{H}$  NMR analysis did not show the presence of any cyclized products (Scheme 2). This suggests either the radical driven cross-coupling is even faster than the 5-exo-trig process or much more likely the aryl halide activation step proceed via OA/RE cycle with Cu(I)/Cu(III) intermediates.



**Scheme 2.** Radical clock experiments

**2.4. Overall mechanistic insights.** Collectively, the results gathered by RPKA show apparent zero-order in both **2a** and NaOH, approximately first order in **1a** and CuI and positive order in ligand. Given the transient nature of Cu(III), it is likely the amine binding and subsequent deprotonation happens prior to a turnover-limiting oxidative addition / reductive elimination process (a radical process being ruled out by the radical clock experiments). The most important step kinetically is therefore a transformation involving **1a** and a Cu+Ligand complex which is already loaded with deprotonated **2a**. In addition, ligand saturation kinetics are suggestive of the presence of an off-cycle pre-equilibrium leading to catalytically inactive cuprates of the form  $[\text{Cu}(\text{NR}_2)_2]^-$ . As such this system adheres well to previously reported mechanistic models for copper-catalyzed Ullmann coupling and related systems.<sup>[21,28,30]</sup> A catalytic cycle consistent with literature proposals, but modified to incorporate a  $\text{L}_2\text{X}_2$  tetramide ligand in which one of the LX units can readily associate/dissociate from the copper center is put forward in Scheme 3. The coordination behavior of tetramide ligands with Cu(I) remains speculative at this stage.



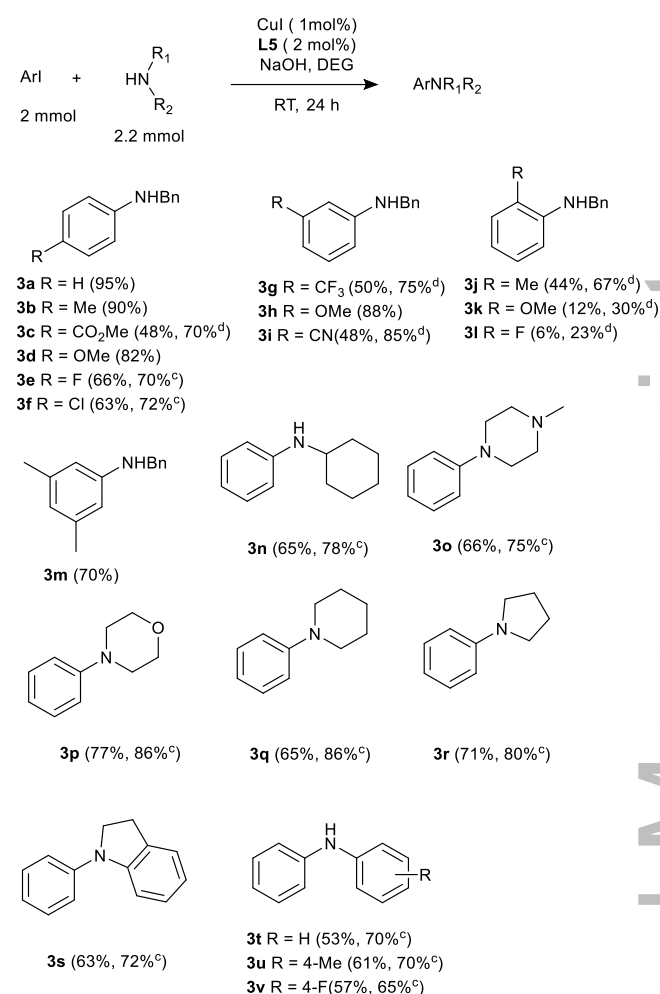
**Scheme 3.** Proposed schematic catalytic cycle.

**3. Substrate scope.** With a better understanding of the catalytic cycle and parameters affecting the reaction rate, mechanistically guided modification of reaction conditions can be applied to the current system. Specifically: (i) ligand **L5** was selected due to fastest reaction rate during the reaction course amongst all ligands tested (Section 2.1); (ii) lower equivalence of amine and base could be employed without any negative impact on the yields or reaction rate (Section 2.2); and (iii) ligand was employed in a 1:2 stoichiometry relative to CuI as a result of the non-linear relationship between reaction rate and ligand loading (Section 2.3).

To this point, all the cross-coupling reactions studied in this work have involved unhindered, relatively reactive primary amines and unsubstituted iodobenzene. Thus, to explore the generality and limitation of this methodology, studies using a much

wider range of aryl iodides and amines have been undertaken with the results summarized in Table 2.

**Table 2.** Substrate scope for tetramide promoted copper-catalyzed cross-coupling<sup>a,b</sup>



<sup>a</sup> Reaction conditions: aryl halide (2 mmol), amine (2.2 mmol), CuI (0.02 mmol), **L5** (0.04 mmol), NaOH (2.2 mmol), DEG (2 mL), RT, 24 h. <sup>b</sup> Isolated yields are quoted. <sup>c</sup> CuI (0.04 mmol) and **L5** (0.08 mmol) were used. <sup>d</sup> CuI (0.1 mmol), **L5** (0.2 mmol) were used.

Aryl iodides bearing a variety of function groups such as alkyl, ether, ester, halogen, trifluoromethyl and nitrile were well-tolerated under standard conditions (**3b** – **3m**). In particular, substrates with electron-rich (Me and OMe) and moderately electron deficient (halogen) substituents at the *para* or *meta* position reacted smoothly (typical 70 - 90% yield). Strong electron deficient groups, such as CO<sub>2</sub>Me, CF<sub>3</sub> and CN, proved compatible but afforded lower yields due to incomplete conversion: This is consistent with previous literature reports, and supports assignment of the rate determining step as oxidative addition of the aryl halide.<sup>[8,13]</sup> Increasing the catalyst loading to 5 mol% CuI, 10 mol% **L5** led to improved yields of 70 – 85% in these cases (**3c**, **3g**, **3i**). Attempts to increase the



yield further by raising the reaction temperature to 80°C gave only marginal improvements (for example, 75% yield for **3s**), presumably due to the increase in the rate of the coupling reaction being countered by higher rates of catalyst deactivation.

Ortho-substituted aryl iodides proved to be more challenging substrates, most likely due to unfavorable steric interactions, and gave poor to moderate yields even with increased catalyst loading (**3j**, **3k**, **3l**).

Five- and six-membered cyclic secondary (hetero)cyclic amines, including cyclohexylamine (**3n**), *N*-methylpiperazine (**3o**), morpholine (**3p**), piperidine (**3n**), pyrrolidine (**3r**), and indoline (**3s**) were coupled in good yield (typically  $\geq 70\%$ ). Remarkably, it was also possible to couple more challenging aryl amines bearing electron donating (**3t**, **3u**) or even electron withdrawing groups (**3v**).

The scalability of this protocol was evaluated in a larger 10 mmol reaction between **1a** and **2a**. This afforded the desired pure product **3a** in 88% (1.61 g) isolated yield, further demonstrating the practical utility of the protocol.

Attempts to use aryl bromides in place of aryl iodides were initially unsuccessful under these conditions. However, raising the temperature to 80°C and the catalyst loading to 10% CuI, 20% **L5** gave 65% yield of **3a** (see Table S2). In our previous ‘same-excess’ experiments we showed how *in-situ* generated water from use of NaOH only has a minor detrimental role in terms of catalyst deactivation (Section 2.2). However, in this case since aryl bromide activation is more sluggish than that of aryl iodide, the deactivation pathway is likely to be much more competitive. An increased rate of catalyst deactivation at 80°C would explain the failure of the reaction to proceed to completion. In order to mitigate against this we swapped to the heterogeneous base  $K_3PO_4$  in which the generated protons can be trapped in a hydrogen phosphate solid, therefore slowing water induced catalyst deactivation.<sup>[22]</sup> Using this approach the yield of **3a** could be boosted to 90%. Attempts to extend the protocol further to aryl chlorides were unsuccessful.

## Conclusion

In summary, we have developed a novel, efficient, and practical reaction system for copper-catalyzed amination of aryl iodides with aliphatic and aryl amines at room temperature using taramide ancillary ligands. The coupling reaction employs cheap and readily available pre-catalyst, ligand, and base. Moreover, this protocol overcomes many current limitations often associated with Ullmann coupling: it

can be run with low catalyst loadings (in most cases 1 mol% CuI and 2 mol% ligand), does not require the use of excess amine (just 1.1 equivalence), gives excellent conversions at room temperature, is fully homogeneous, and displays improved tolerance to air and moisture. These advantages make it potentially attractive for both academic and commercial applications.

Moreover, detailed kinetic studies using reaction progress kinetic analysis (RPKA) protocols have provided insight into the factors influencing the reaction rate in terms of impact of ligand structure, reactant / catalyst dependence and catalyst (in)stability. Such information had been employed in a quality-by-design approach towards catalytic system optimization in this work, and in addition provides a platform for future development of the catalytic system.

## Experimental Section

**General procedure for the copper-catalysed cross-coupling (Table 2):** CuI (1-5 mol%), **L5** (2-10 mol%), amine (2.2 mmol), aryl iodide (2.0 mmol), NaOH (88 mg, 2.2 mmol) and DEG (4 mL) was added to a reaction vial charged with Teflon-coated magnetic stir bar under a nitrogen atmosphere. The vial was capped and stirred at room temperature for 24 hours. The reaction mixture was then diluted with DCM and washed with water and brine. The organic phase was dried over  $MgSO_4$  and concentrated *in vacuo*. The product was isolated and purified using silica chromatography if required, and the resulting product characterised using  $^1H$  and  $^{13}C$  NMR (see SI for full data).

Experimental details for the synthesis and characterisation of all ligands (**L1-L8**), and full details of the kinetic measurement protocols and resulting data are provided in the SI.

## Acknowledgements

We thank Pete Haycock for help with NMR analysis.

## References

- [1] R. Gosmini, V. L. Nguyen, J. Toum, C. Simon, J. M. G. Brusq, G. Krysa, O. Mirguet, A. M. Riou-Eymard, E. V. Boursier, L. Trottet, P. Bamborough, H. Clark, C. W. Chung, L. Cutler, E. H. Demont, R. Kaur, A. J. Lewis, M. B. Schilling, P. E. Soden, S. Taylor, A. L. Walker, M. D. Walker, R. K. Prinjha and E. Nicodème, *J. Med. Chem.*, **2014**, *57*, 8111–8131.
- [2] H. Zhou, J. Chen, J. L. Meagher, C. Y. Yang, A. Aguilar, L. Liu, L. Bai, X. Cong, Q. Cai, X. Fang, J. A. Stuckey and S. Wang, *J. Med. Chem.*, **2012**, *55*, 4664–4682.
- [3] J. Chen, H. Zhou, A. Aguilar, L. Liu, L. Bai, D. McEachern, C. Y. Yang, J. L. Meagher, J. A. Stuckey and S. Wang, *J. Med. Chem.*, **2012**, *55*, 8502–8514.

- [4] G. Evano, N. Blanchard and M. Toumi, *Chem. Rev.*, **2008**, *108*, 3054–3131.
- [5] Y. Abiko, A. Matsumura, K. Nakabayashi and H. Mori, *Polymer.*, **2014**, *55*, 6025–6035.
- [6] H. Murakami, R. Nishiide, S. Ohira and A. Ogata, *Polymer.*, **2014**, *55*, 6239–6244.
- [7] I.P. Beletskaya and A. V. Cheprakov, *Organometallics*, **2012**, *31*, 7753–7808.
- [8] J. Gao, S. Bhunia, K. Wang, L. Gan, S. Xia and D. Ma, *Org. Lett.*, **2017**, *19*, 2809–2812.
- [9] Q. Cai and W. Zhou, *Chinese J. Chem.*, **2020**, *38*, 879–893.
- [10] S. Bhunia, G. G. Pawar, S. V. Kumar, Y. Jiang and D. Ma, *Angew. Chemie - Int. Ed.*, **2017**, *56*, 16136–16179.
- [11] A. Shafir and S. L. Buchwald, *J. Am. Chem. Soc.*, **2006**, *128*, 8742–8743.
- [12] C. T. Yang, Y. Fu, Y. B. Huang, J. Yi, Q. X. Guo and L. Liu, *Angew. Chemie - Int. Ed.*, **2009**, *48*, 7398–7401.
- [13] Q. A. Lo, D. Sale, D. C. Braddock and R. P. Davies, *ACS Catal.*, **2018**, *8*, 101–109.
- [14] Q. A. Lo, D. Sale, D. C. Braddock and R. P. Davies, *European J. Org. Chem.*, **2019**, 1944–1951.
- [15] I. D. Williams, S. F. Pedersen, K. B. Sharpless and S. J. Lippard, *J. Am. Chem. Soc.*, **1984**, *106*, 6430–6431.
- [16] K. Narasaka, N. Iwasawa, M. Inoue, T. Yamada, M. Nakashima and J. Sugimori, *Chem. Lett.*, **1989**, *15*, 793–796.
- [17] Y. Hayashi and K. Narasaka, *Chem. Lett.*, **1989**, *18*, 793–796.
- [18] A. Casitas and X. Ribas, *Chem. Sci.*, **2013**, *4*, 2301–2318.
- [19] A. Casitas, A. E. King, T. Parella, M. Costas, S. S. Stahl and X. Ribas, *Chem. Sci.*, **2010**, *1*, 326–330.
- [20] W. Chen, Y. Liu and Z. Chen, *European J. Org. Chem.*, **2005**, 1665–1668.
- [21] S. Sung, D. Sale, D. C. Braddock, A. Armstrong, C. Brennan and R. P. Davies, *ACS Catal.*, **2016**, *6*, 3965–3974.
- [22] G. J. Sherborne, S. Adomeit, R. Menzel, J. Rabeah, A. Brückner, M. R. Fielding, C. E. Willans and B. N. Nguyen, *Chem. Sci.*, **2017**, *8*, 7203–7210.
- [23] C. Meyers, B. U. W. W. Maes, K. T. J. J. Loones, G. Bal, G. L. F. F. Lemièrre and R. A. Dommissie, *J. Org. Chem.*, **2004**, *69*, 6010–6017.
- [24] J. W. Tye, Z. Weng, A. M. Johns, C. D. Incarvito and J. F. Hartwig, *J. Am. Chem. Soc.*, **2008**, *130*, 9971–9983.
- [25] J. W. Tye, Z. Weng, R. Giri and J. F. Hartwig, *Angew. Chemie - Int. Ed.*, **2010**, *49*, 2185–2189.
- [26] K. A. Cannon, M. E. Geuther, C. K. Kelly, S. Lin and A. H. R. Macarthur, *Organometallics*, **2011**, *30*, 4067–4073.
- [27] D. G. Blackmond, *J. Am. Chem. Soc.*, **2015**, *137*, 10852–10866.
- [28] R. Giri, A. Brusoe, K. Troshin, J. Y. Wang, M. Font and J. F. Hartwig, *J. Am. Chem. Soc.*, **2018**, *140*, 793–806.
- [29] S. Shekhar, P. Ryberg, J. F. Hartwig, J. S. Mathew, D. G. Blackmond, E. R. Strieter and S. L. Buchwald, *J. Am. Chem. Soc.*, **2006**, *128*, 3584–3591.
- [30] E. R. Strieter, B. Bhayana and S. L. Buchwald, *J. Am. Chem. Soc.*, **2009**, *131*, 78–88.
- [31] R. Giri and J. F. Hartwig, *J. Am. Chem. Soc.*, **2010**, *132*, 15860–15863.

## RESEARCH ARTICLE

Tartramide Ligands for Copper-Catalyzed  
N-Arylation at Room Temperature*Adv. Synth. Catal.* **Year**, *Volume*, Page – Page

Xuerui Ma, Robert P. Davies\*

